SSRG International Journal of Industrial Engineering
ISSN: 2349 – 9362 / https://doi.org/10.14445/23499362/IJIE-V13I2P102

Volume 13 Issue 2, 10-23, May-Aug 2026

Original Article

Impact of Frequency on Square Plate

Chukwuemeka Joshua Okafor[1], Adedayo Emmanuel AINA[2], Rebecca Bolaji KALASUWE[3], Damilola ADEBAYO[4]

[1]*School of Computing, Engineering, and Digital Technologies, Teesside University, United Kingdom.*
[2]*University of Greenwich, England, United Kingdom.*
[3]*Teesside University, United Kingdom.*
[4]*Northern Arizona University, United States of America.*

[1]*Corresponding Author : okaforjoshua180@gmail.com*

Received: 09 June 2026 Revised: 18 July 2026 Accepted: 07 August 2026 Published: 28 August 2026

Abstract - *Parts A and B form this report. Part A investigates the influence of frequency on a square plate using Warburton's theorem. A Modal evaluation is performed on a fixed square plate having a length and width of 1000 mm x 1000 mm and a thickness of 1.75mm employing Siemens NX, version 12. SOL 103 real Eigenvalues is the solver utilized within the program to determine the mode patterns on the plate of the first ten natural frequencies. To correlate the simulation performance analysis with the underlying analytical theory, the first 10 natural frequencies are obtained in excel using Warburton's theory. With the exception of a few differences, the simulation mode forms corroborate Warburton's hypothesis and were near to the analytical predictions. Part B explicitly define background theory of linear and nonlinear analysis. A simulation of the linear and nonlinear behavior of a guttering bracket was also carried out to examine the behavior of the model. The analysis shows that for an applied force of 100 N, the maximum displacement for both linear and nonlinear is within 5 mm. While the stress acted on the material shows that the true stress is the nonlinear analysis, as it shows the nodal stress concentration.*

Keywords *- Square plate, Warburton's Theorem, Finite Element Analysis (FEA), Natural Frequencies.*

1. Introduction

1.1. Background

Following the various practical applications, there is quite a variety of research devoted to vibrating square plates following Euler's first numerical approach in 1766. Controlling vibrations is an important component in the structural design process since excessive vibration can cause difficulties spanning from noise and vibration disturbance to structural collapse. As a result, it is critical to conduct a vibration profile analysis for metal plates to forecast and ensure that vibration responses, forces, stresses, and radiated sound are within an acceptable threshold under normal operating circumstances (Brunesi *et al*., 2014; Dickinson and Di Blasio, 1986; Nowacki, 1963).

Hence, Okafor, Adeniran and Adeniran (2025), Adorno and Palazotto (2023) and Warburton and Edney (1984) used the Rayleigh-Ritz approach in finding the natural frequencies in transverse vibration of thin plates with elastically constrained edges by employing the appropriate vibration mode forms of a beam with classical boundary conditions as presumed variables (Dickinson and Di Blasio, 1986; Laura, 1997; Zhou, 1995a; Zhou, 1995b; Okafor, 2024). The various modes of vibration of a square plate describe the nodal pattern in it. Figure 1 shows the nodal pattern in the m- direction and Figure 2 shows the nodal pattern in the n- direction.

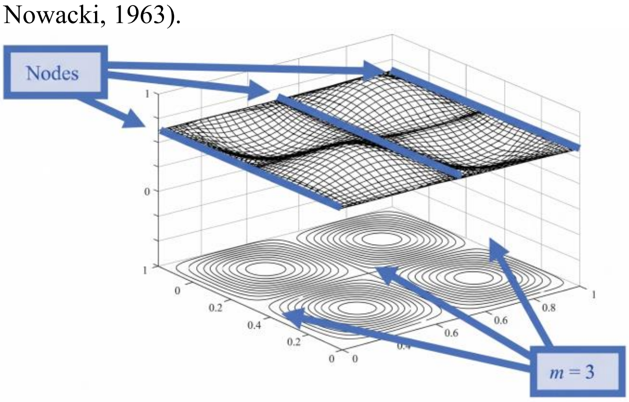

Fig. 1 m- Direction of the nodal pattern.

Source: Hughes and Tezduyar (1981)

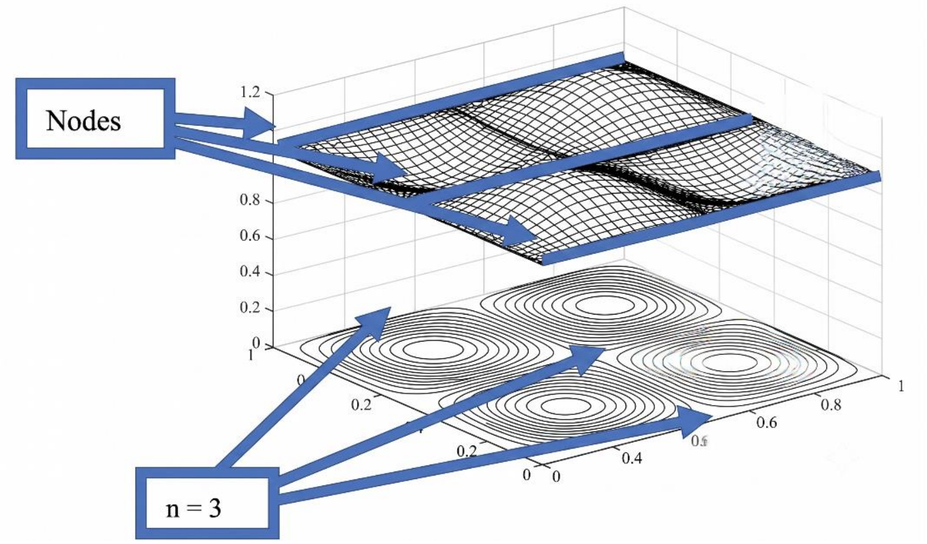

Fig. 2 n- Direction of the nodal pattern

Source: Hughes and Tezduyar (1981)

Also, the Mindlin plate theory is used to solve the mathematical model stress deformation analysis of the plates. It is deemed to be an extension of the Kirchhoff-love plate and accurate because it considers the shear deformation of the plate (Ike, 2019; Okafor, 2025).

1.2. Lanczos and Householder Process

Cornelius Lanczos developed the Lanczos method, which he modified from the power technique and utilized to determine the m Eigenvalues as well as Eigenvectors of a n x n Hermitian matrix (Lanczos, 1950). Furthermore, even after the 1970s, engineers were unable to use the technique and adapt it to extremely big buildings with dynamic loading (Ojalvo and Newman, 1970).

According to Allerdt *et al*. (2020), the Householder and QR factorization techniques were superior for solving eigenvalue issues with general matrices (Welch-Phillips, 2020; Williamson and Williamson, 2021). Once computers could solve large matrices, the Lanczos technique beat the general algorithms. The Householder method and the Lanczos method are very similar and can be used to accomplish the same objective because they have the same properties for eigenvalue convergence (Ahmed, 2023; Brunesi *et al*., 2014; Sau and Heyde, 1979). The Lanczos technique, on the other hand, is better for the ten lowest eigenvalues.

1.3. Objective

- To model a square plate and apply Warburton's theory.
- To use FEM analysis to investigate and simulate the model.
- To evaluate the theoretical values of the first ten natural frequencies in excel.

2. Methodology

2.1. Materials

This study employed thorough checks on different journals, archives, articles, conferences, and magazines to understand the vibration theory of a thin metal square plate with all sides fixed.

2.1.1. Software Used

The Siemens NX, version 12.0, was used to design the Square Plate, and it is versatile enough to handle the various modeling that the tools for Computer-Aided Design (CAD) and Computer-Aided Engineering (CAE) will handle.

2.1.2. Material Selection and Properties

The material selected for this model is steel. This is due to its application and functions in the global industry. Steel is widely used in most works because of its high tensile strength, durability, rust resistance, conductivity, luster, and many more. Other properties, such as young modulus, poison's ratio, density, and others, are presented in Table 2.1.

Table 1. Properties of Steel material.

Features	VALUE	UNIT
Young Modulus	2.10E+05	N/mm^2
Poison's ratio	0.3	
Gravity (g)	9.81E+03	N
Density (p)	7.83E-05	g/mm^3
Thermal conductivity	25	W/m^0C

2.2. Methods

With the use of the NX Simcenter, a square plate model was created with dimensions 1000 mm by 1000 mm. Then the model was extruded to a thickness of 1.75 mm, and then apply the pre-post FEM method was applied to analyze the square plate with all sides fully fixed to obey the Warburton theory (Cattari, 2022; Chan, 1988; Datta and Rakesh, 2010). The model was created with the "new" command displayed on the home tab, followed by the model, set the model's name as "Square plate" and save it in a folder as shown in Figure 3.

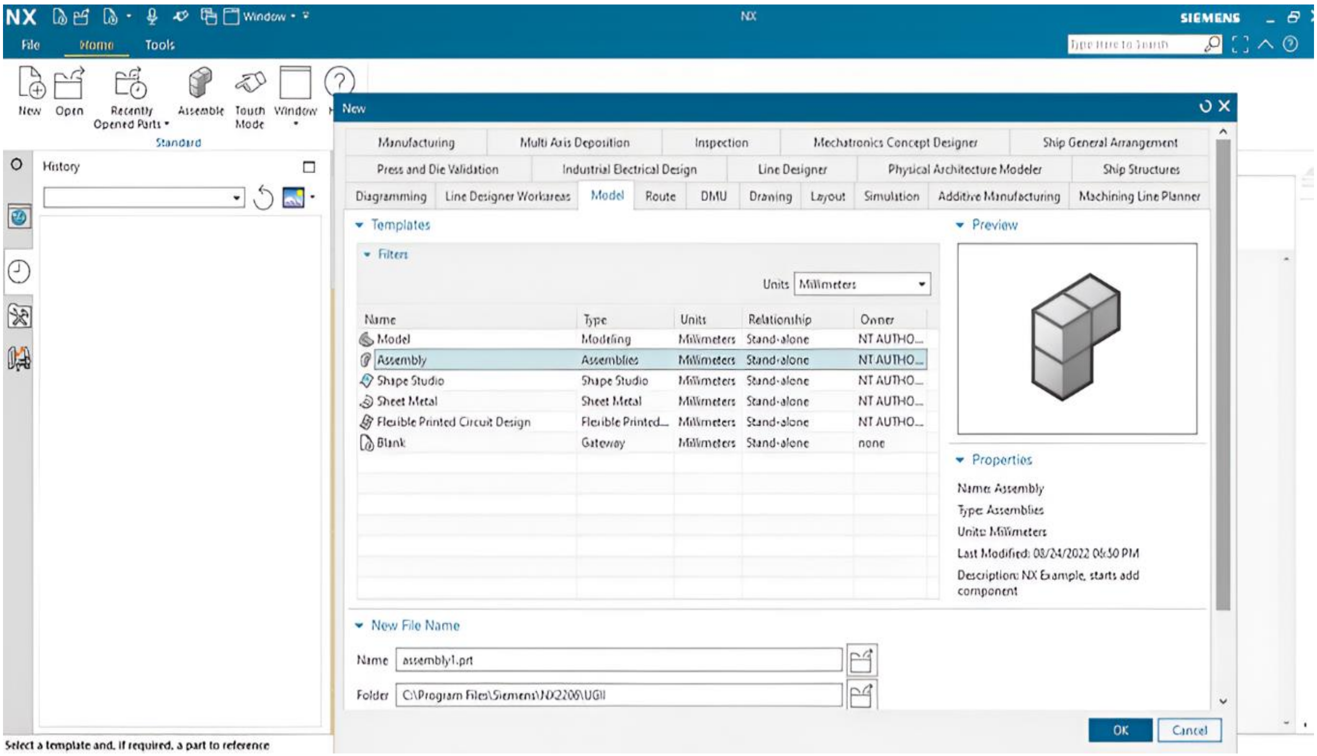

Fig. 3 Explains all the NX Simcenter steps in creating the model

After creating the model, on the home tab- application and then pre/post as shown in Figure 4, which helps to analyze the difference and compare them with Warburton theory (Lancoz- Eigenvalue solver).

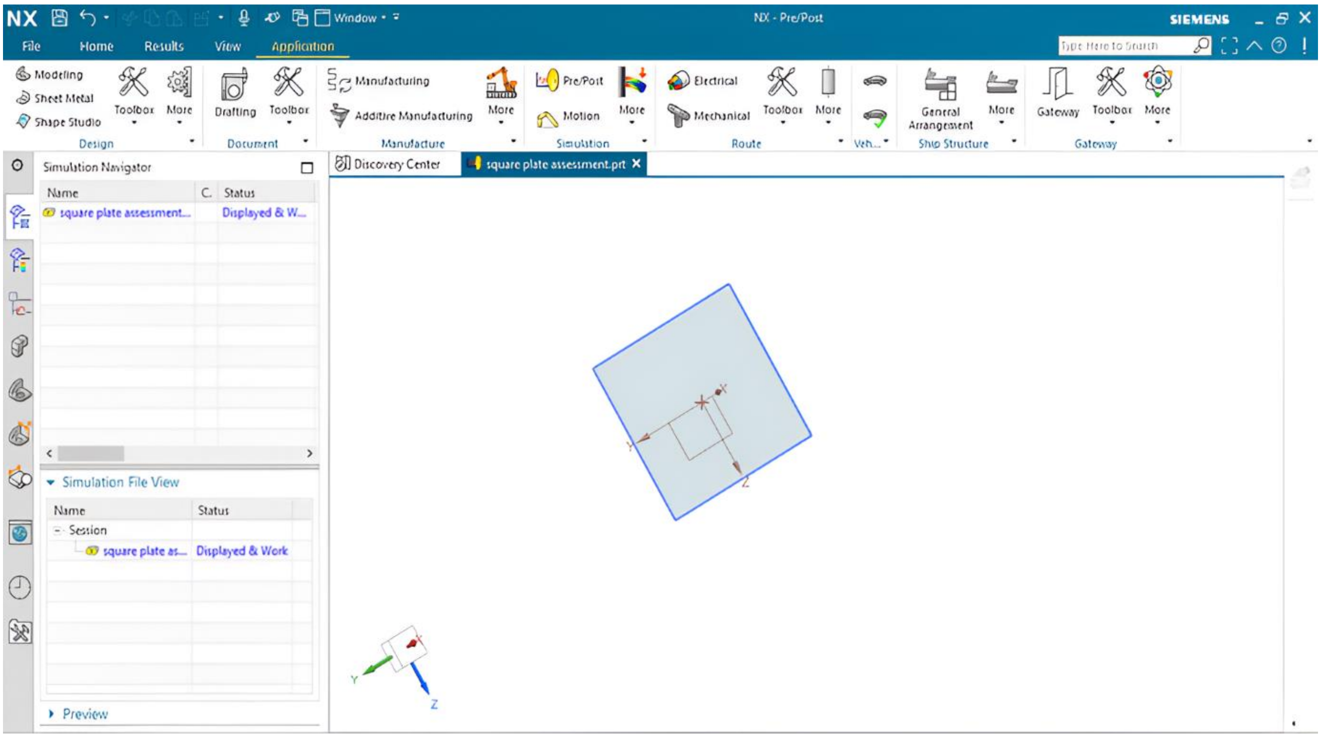

Fig. 4 Pre/post–application of the model

Once the Pre/Post is created, then the Fem and simulation part files can be generated from the idealized part file. The fem file consists of mesh data, materials, and physical properties, while the Simulation file includes the boundary conditions and specific data solution solvers (Li, 2023; Mackerle, 1997; Nanetti and Benvenuti, 2021). The solution type selected is the SOL 103 Real Eigenvalues, as can be seen in Figure 5. Also, the real eigenvalue method used is the Lanczos and householder solver, which helps simplify the analysis into different modes of frequency acting upon the square plate.

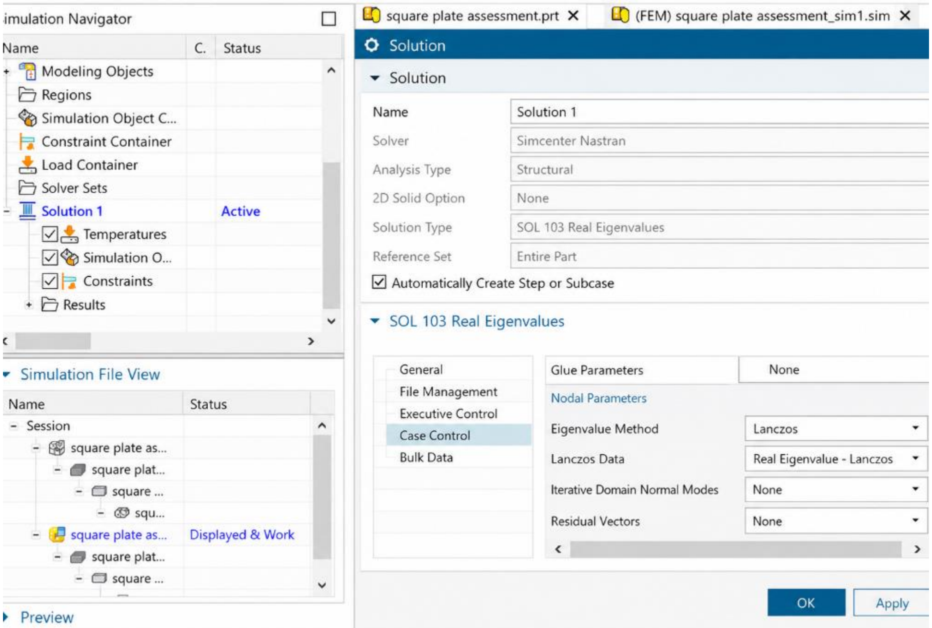

Fig. 5 Image showing the Fem and Sim file creation with SOL103 real eigenvalue

After creating this part file and simulation, on the idealized parts, promote the model so that modifications can be done, followed by mid-surfacing, as seen in Figure 6. The mid-surface helps to suppress some features within the model so that a mesh can be applied to the model.

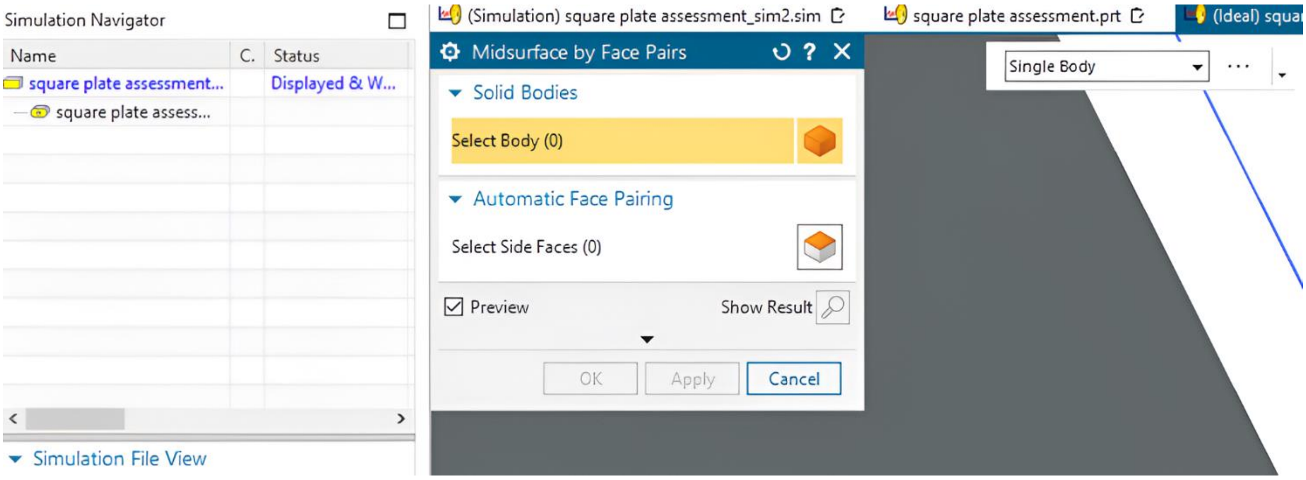

Fig. 6 Mid-surfacing of the Model

Hence, a mesh can be created (2-D Mesh), and the material assigned to the model is steel. This can be seen from Figure 7 (a), where the element size is set at 100 mm with element properties type as CQUAD4, while (b) is the Destination collector where the material was assigned to the model,

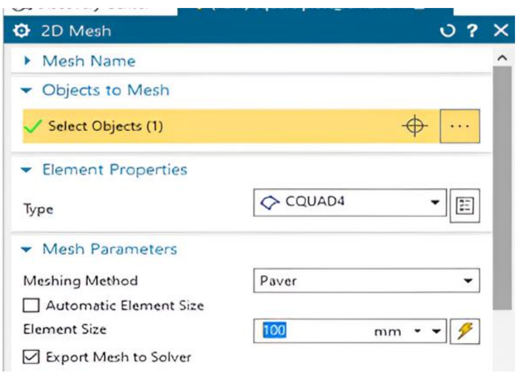

Fig. 7 (a) 2-D Mesh

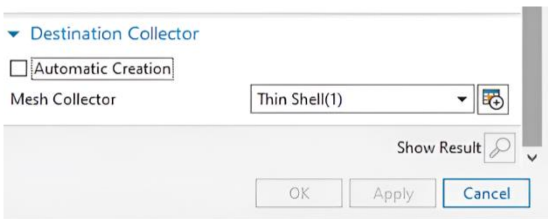

(b) Material selection

Once the meshing is completed, save it on the sim file and make the sim file the displayed and worked part (Xue, 2023; Zhao, 2020; Zhou, 1995a; Zhou, 1995b). From the sim, the worked part, home- constraint type – fixed constraints (Figure 8), and pick all four sides of the square plate to apply the boundary conditions. When completed on the simulation navigator, right-click the mouse on the solution and solve (Nowacki, 1963; Ojalvo and Newman, 1970; Osadebe, 1997; Reddy, 1984; Sau and Heyde, 1979). Allow the process to generate the analysis and evaluations for the model, after which, view the results generated.

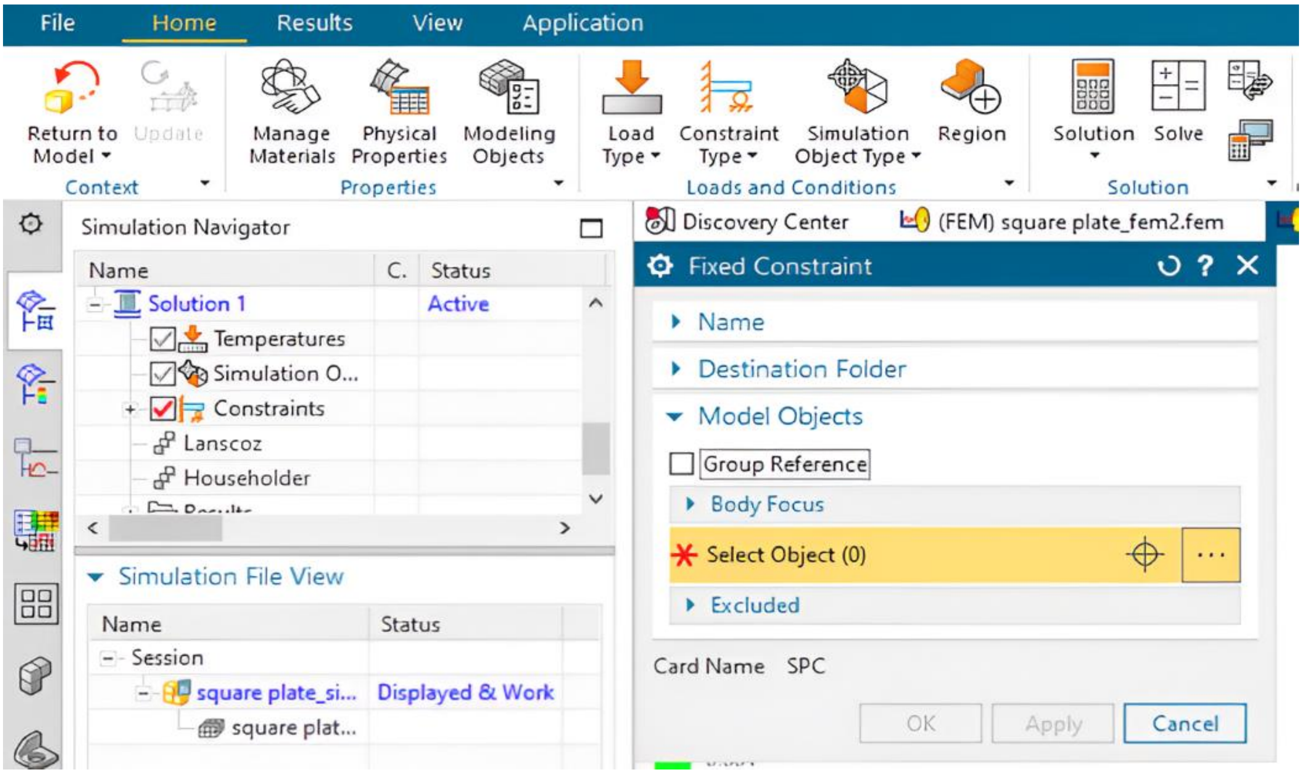

Fig. 8 Applying a constraint on the model

2.3. Plate Geometry

To explain plate interactions, several theories and models were created. Kirchhoff theory, Mindlin theory (Do *et al*., 2020; Geng *et al*., 2001; Hendriks and Rots, 2013; Ike, 2019). Reissner theory, Shimpi improved theory, Reddy theory, and Osadebe plate model are a few of them (Lanczos, 1950; Laura, 1997; Sifakis and Barbic, 2012; Warburton and Edney, 1984). In this study, Warburton is an infinitesimal linear theory appropriate for thin orthotropic and isotropic surfaces. The basic equations and techniques of solution will be presented before discussing the various boundary conditions. The vibration form for a square plate with sides of lengths a and b must meet the boundary criteria for fully fixed edges according to(Ike, 2019) ,

$$\frac{\delta^4 w}{\delta x^4} + 2\frac{\delta^4 w}{\delta x^2 \delta y^2} + \frac{\delta^4 w}{\delta y^4} + \frac{12p(1-\sigma^2)}{Egh^2}\frac{\delta^2 w}{\delta x^2} \qquad (1)$$

Where w is the displacement of any point on the x, and y-axis with time t, and is given as

$$w = W \sin wt \qquad (2)$$

w is the transverse displacement of the plate on a particular area, w =2πf

The criteria of fixity allow us to write:

- For no displacement:

$$w(x,y,t) = 0 \; for \; x = 0, x = a \qquad (3)$$

$$w(x,y,t) = 0 \; for \; y = 0, y = b \qquad (4)$$

- For no moment

$$\delta\frac{\delta^L(x,y,t)}{\delta^2 x} = 0 \; for \; x = 0, x = a \qquad (5)$$

$$\delta\frac{\delta^2(x,y,t)}{\delta^2 y} = 0 \; for \; y = 0, y = b \qquad (6)$$

- For Strain analysis

$$\varepsilon_{xx} = z\frac{\partial\theta_x}{\partial_x} \qquad (7)$$

$$\varepsilon_{yy} = z\frac{\partial\theta_y}{\partial_y} \qquad (8)$$

$$\varepsilon_{zz} = 0 \qquad (9)$$

$$Y_{xy} = z(\frac{\partial\theta_x}{\partial_x} + \frac{\partial\theta_y}{\partial_y}) \qquad (10)$$

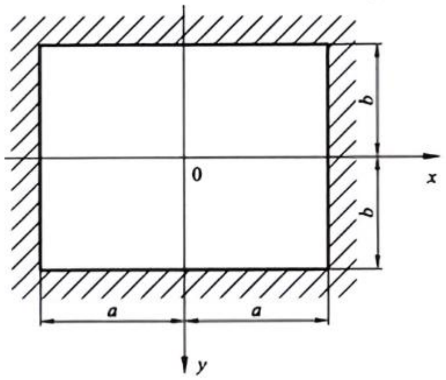

Fig. 9 Illustration of a uniformly fixed square plate (Imrak and Fetvaci, 2009)

2.4. Expression of the Square Plate Frequency

According to the following coefficient, the frequency equation is obtained from Warburton's theory of a fully fixed rectangular plate, and a similar approach was adopted for the square plate.

$$G_x = \left(m - \tfrac{1}{2}\right) \tag{11}$$

$$G_y = \left(n - \tfrac{1}{2}\right) \tag{12}$$

Where m and n are the numbers of nodal lines in the X and Y directions, respectively, G_x and G_y are the functions of m and n in frequency representation.

$$H_y = \left(n - \tfrac{1}{2}\right)^2 \left(1 - \frac{2}{\left(n-\frac{1}{2}\right)\Pi}\right) \tag{13}$$

$$H_x = \left(m - \tfrac{1}{2}\right)^2 \left(1 - \frac{2}{\left(m-\frac{1}{2}\right)\Pi}\right) \tag{14}$$

Where H_x, H_y, J_x, and J_y are the functions of m and n in the frequency evaluation.

$$J_x = \left(m - \tfrac{1}{2}\right)^2 \left(1 - \frac{2}{\left(m-\frac{1}{2}\right)\Pi}\right) \tag{15}$$

$$J_y = \left(n - \tfrac{1}{2}\right)^2 \left(1 - \frac{2}{\left(n-\frac{1}{2}\right)\Pi}\right) \tag{16}$$

With a non-dimensional frequency factor λ, the proportionality frequency is obtained.

$$\lambda^2 = \frac{pa^4(2\Pi f)^2 12(1-a^2)}{\Pi E h^2 g} \tag{17}$$

While for a boundary condition with free, fixed sides, its frequencies are obtained using the expression.

$$\lambda^2 = G_x{}^4 + G_y{}^4 \frac{a^4}{b^4} + \frac{2a^2}{b^2}\left(\upsilon H_x H_y + (1-\upsilon) J_x J_y\right) \tag{18}$$

Hence, the frequency factor is calculated with the ratio a/b and the frequency obtained by

$$F = \frac{\lambda h \Pi}{a^2}\left(E\, x \frac{g}{48\rho(1-\upsilon^2)}\right)^{\frac{1}{2}} \tag{19}$$

3. Result and Discussion

3.1. FEM Simulation Result

The nodal pattern in a fixed plate with frequency applied to it, according to Warburton's hypothesis, will manifest itself in a circular form for the first ten natural frequencies or modes, with the help of the Lanscoz, as shown in Figure 10.

The nodal pattern on the plate will alter and take on distinct forms as the frequency increases. This is corroborated by the Siemens NX simulation findings in this study (Bathe and Cimento, 1980; Bhavikatti, 2005; Brunesi *et al.*, 2014). Table 2 depicts the simulation model of Frequency and von mises stress exacted on the square plate, which shows the first ten natural frequencies and stress, including their inherent modes (Lancoz solver).

The simulation Frequency results are presented in graphs, and Table 3 shows the analytical method using excel to apply the Warburton equations. When the initial natural frequency generated a circular nodal pattern on the plate, the mode shape altered as the increase in frequency occurred.

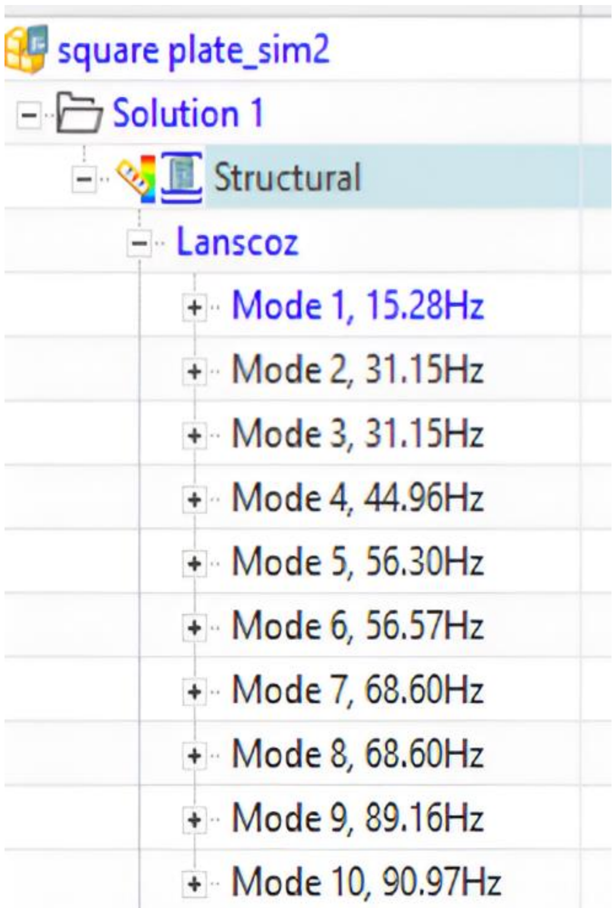

Fig. 10 Result of the FEA Simulation

Table 2. Result analysis of the FEA frequency and stress (Von Misses) of the square plate

Modes	Mode shape of the FEA	Stress of the FEA on the Square Plate
Mode 1 f = 15.67 Hz m= 2 n = 2 = 2.634 MPa	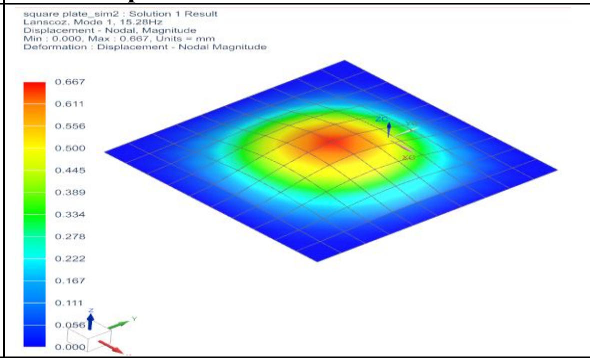	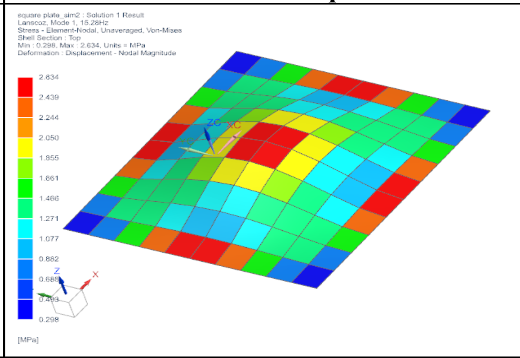
Mode 2 f = 31.99 Hz m= 2 n = 3 = 5.617 MPa	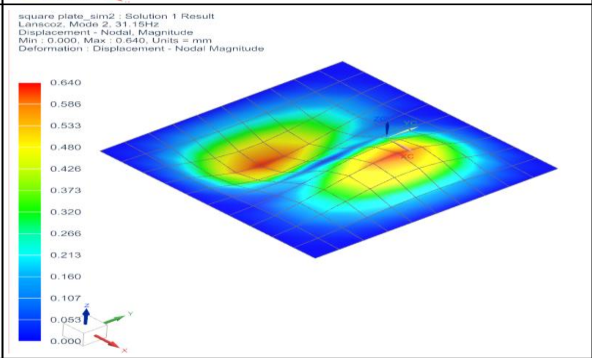	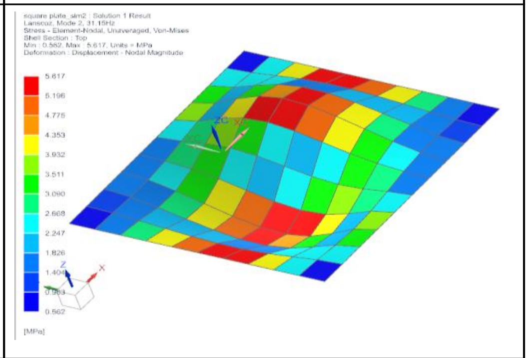
Mode 3 f = 31.99 Hz m = 3 n = 2 = 5.617 MPa	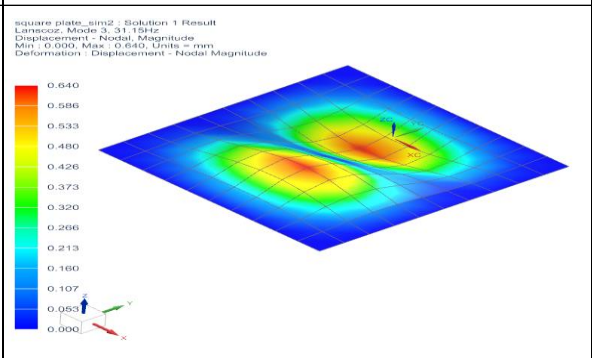	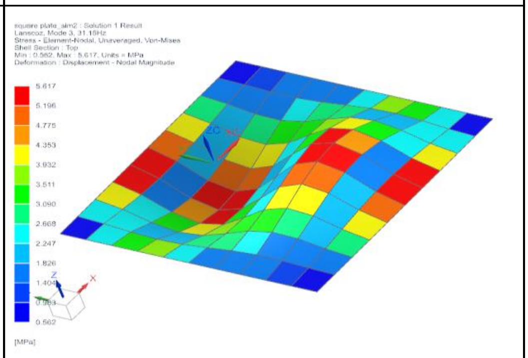
Mode 4 f = 47.04 Hz m = 3 n = 3 = 6.778 MPa	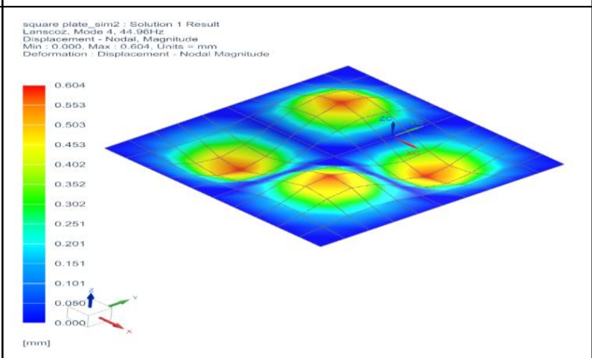	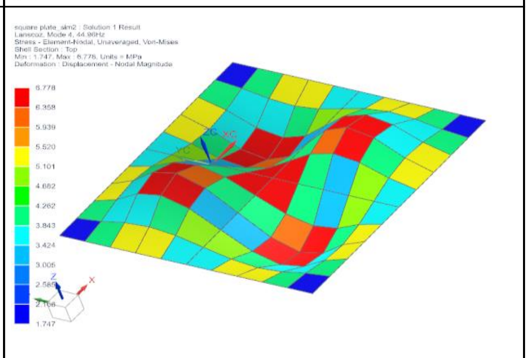
Mode 5 f = 57.42 Hz m = 4 n = 2 = 9.353 MPa	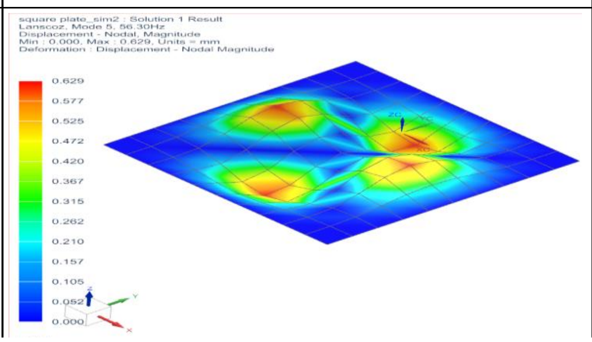	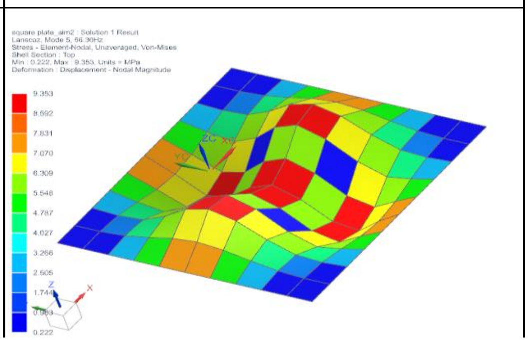

Mode 5 f = 57.42 Hz m = 4 n = 2 = 9.353 σ MPa	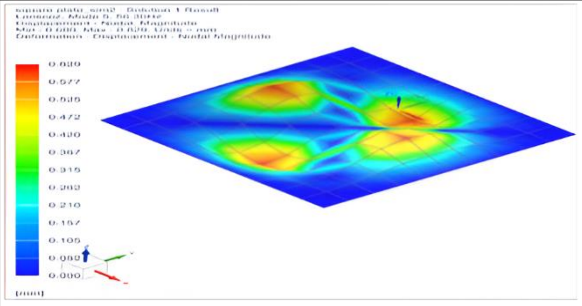	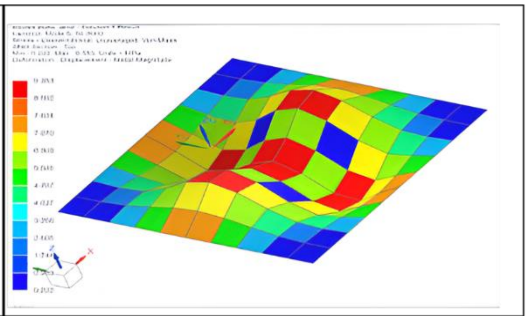
Mode 6 f = 57.42 Hz m = 2 n = 4 = 11.072 σ MPa	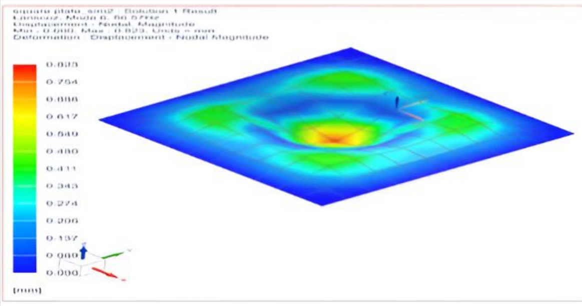	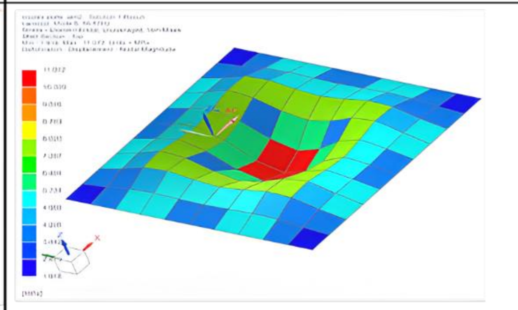
Mode 7 f = 71.72 Hz m = 3 n = 4 = 13.39 σ MPa	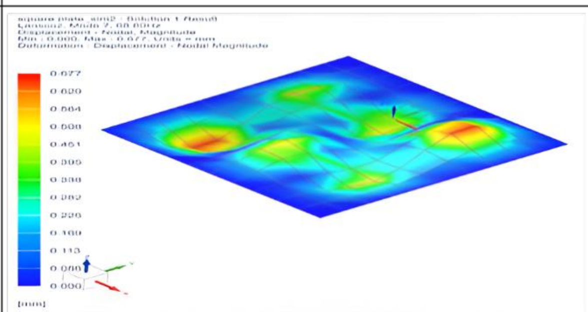	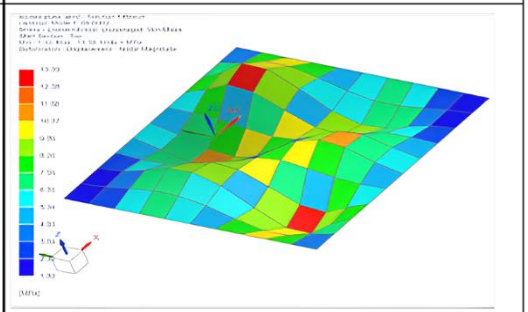
Mode 8 f = 91.54 Hz m = 5 n = 2 = 13.39 σ MPa	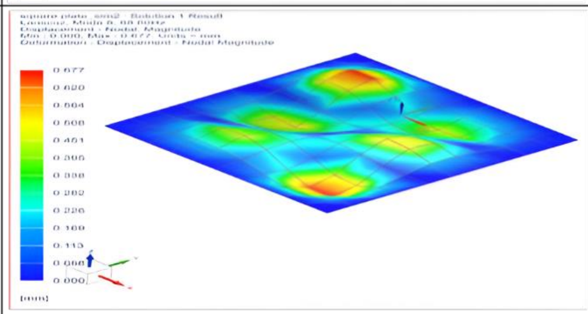	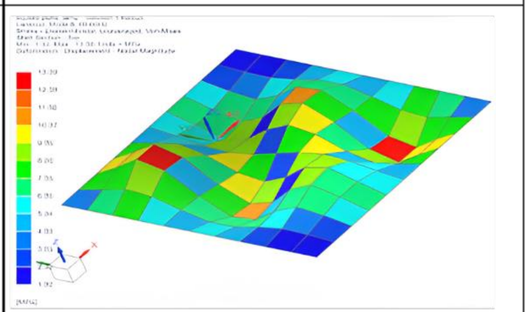
Mode 9 f = 95.51 Hz m = 4 n = 4 = 14.158 σ MPa	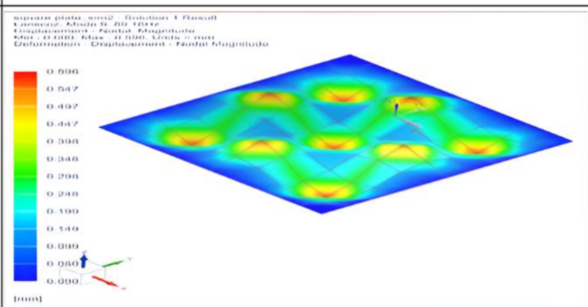	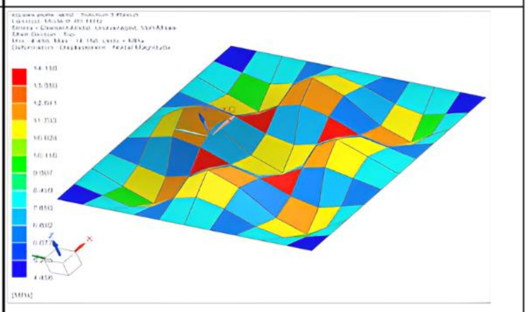
Mode 10 f = 105.49 Hz m = 5 n = 3 = 16.13 σ MPa	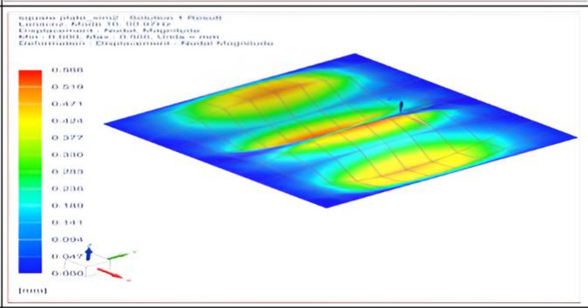	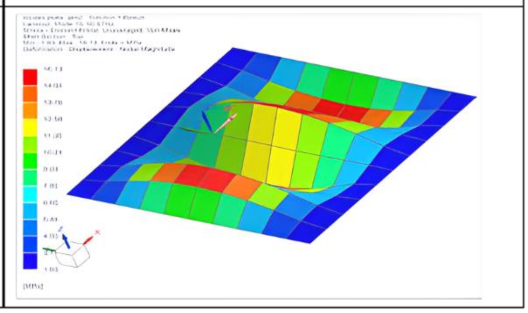

Additionally, Figure 11 compares theoretical and simulation results, demonstrating that there is a positive association between frequency and mode forms as they both grow. Yet, the graph shows that the outcomes are not the same. As the analytical frequency is below the simulated frequency, this is initially seen in mode 7. This is more noticeable in the variables from modes 8, 9, and 10, where the analytical frequency is lower. The range of error among simulation and analytical findings is shown in Table 3. According to the table, the proportion of mistakes in mode 8 is larger than in modes 9 and 10. When utilising software like Siemens NX, a degree of error should be expected. This is not to indicate that the programme is flawed, but rather that there are factors beyond the person's discretion. For instance, the present vibration research shows that as the mode increases, likewise does the specificity of the constraints, potentially causing differences or foibles in the findings. Furthermore, as the model rises, the elements must be further correct when attempting to solve the modelling, potentially causing deficiencies and differentiation among analytical and simulation.

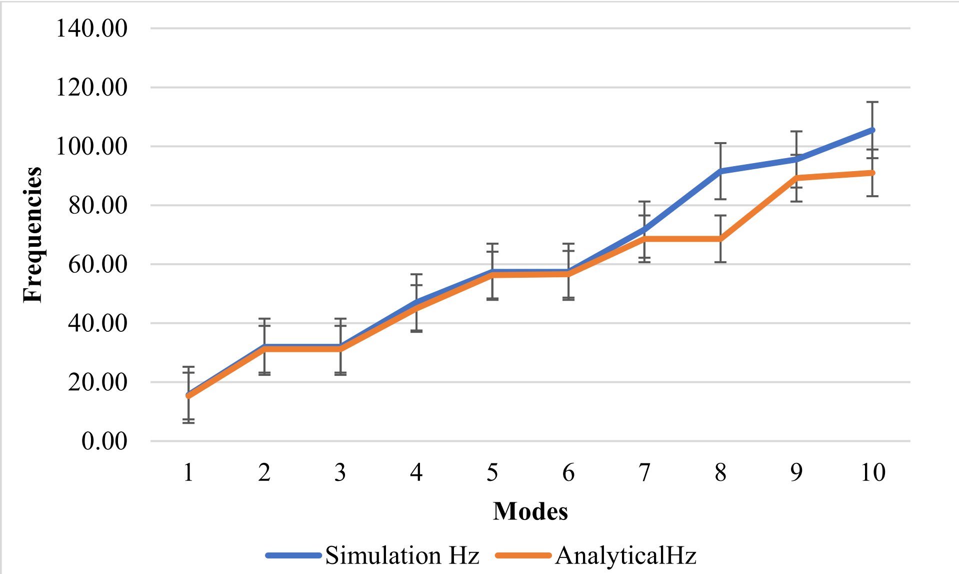

Fig. 11 Graphical representation of Frequencies against mode (comparisom of analytical and simulation result)

Table 3. Analytical result of the first ten Natural Frequency

Number of modes	m	n	Gx	Gy	Hx	Hy	Jx	Jy	λ^2	λ	Frequency
1	2	2	1.5	1.5	1.30	1.30	1.30	1.30	13.48	3.67	15.67
2	2	3	1.5	2.5	1.30	4.66	1.30	4.66	56.19	7.50	31.99
3	3	2	2.5	1.5	4.66	1.30	4.66	1.30	56.19	7.50	31.99
4	3	3	2.5	2.5	4.66	4.66	4.66	4.66	121.53	11.02	47.04
5	4	2	3.5	1.5	10.02	1.30	10.02	1.30	181.08	13.46	57.42
6	2	4	1.5	3.5	1.30	10.02	1.30	10.02	181.08	13.46	57.42
7	3	4	2.5	3.5	4.66	10.02	4.66	10.02	282.50	16.81	71.72
8	5	2	4.5	1.5	17.39	1.30	17.39	1.30	460.16	21.45	91.54
9	4	4	3.5	3.5	10.02	10.02	10.02	10.02	501.00	22.38	95.51
10	5	3	4.5	2.5	17.39	4.66	17.39	4.66	611.10	24.72	105.49

Nevertheless, based on table 3 and Figure 11, modes 8 and 9 does not support this; it is possible that this is an anomaly in the data.

Table 3. % error difference between the analytical and simulation results

Number of modes	m	n	Simulation Hz	Analytical Hz	Gap (Hz)	e %
1	2	2	15.67	15.28	0.39	0.03
2	2	3	31.99	31.15	0.84	0.03
3	3	2	31.99	31.15	0.84	0.03
4	3	3	47.04	44.96	2.08	0.05
5	4	2	57.42	56.30	1.12	0.02
6	2	4	57.42	56.57	0.85	0.02

7	3	4	71.72	68.60	3.12	0.05
8	5	2	91.54	68.60	22.94	0.33
9	4	4	95.51	89.16	6.35	0.07
10	5	3	105.49	90.97	14.52	0.16

3.2. FEA Results vs Literature

Many publications on the mode forms of a square plate at natural frequency have been published. As a result, it is useful to compare such earlier conducted forms to the mode shapes derived by the FEA study, as shown in Figure 4 below. When the mode forms are examined in relation to the reported mode shapes by Imran, Khan, and Badshah, the findings of Hong and Jang (2015; Ike, 2019, Imrak and Fetvaci (2009), and Imran *et al*. (2019) are consistent. The look of the mode forms is consistent, particularly in the first few modes. The latter two modes have a little variance in look, although they have a comparable structure. Its magnitude in the reported modes is more focused in some regions, but the magnitude in the modes gathered for this research is more uniformly distributed throughout an area. It is possible to have numerous causes for this, one of which is to be a meshing variation, implying that one set of findings is collecting a more comprehensive collection of data in a significant increase of vertices.

Table 4. FEA result comparison with published literature (Imran, Khan and Badshah, 2019)

Mode shape of the FEA	Literature Review
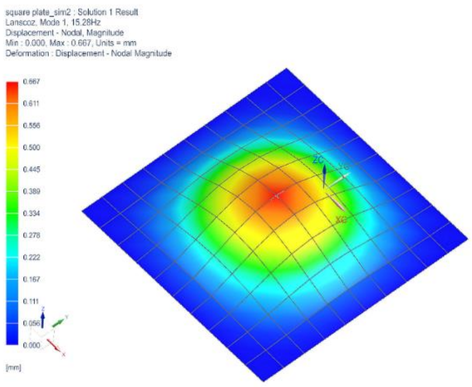	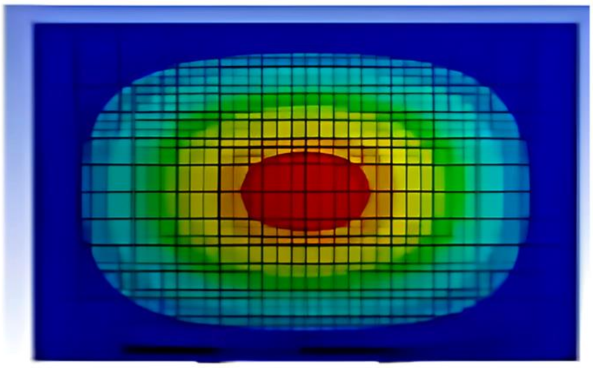
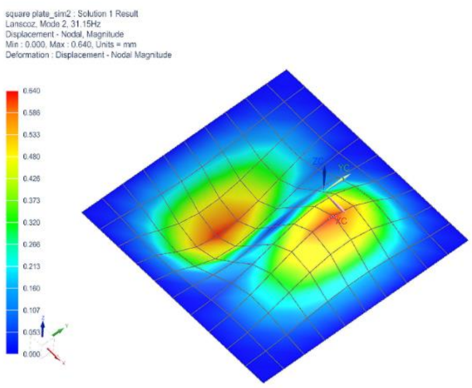	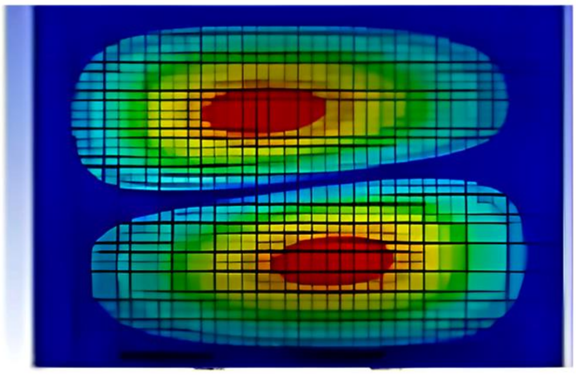
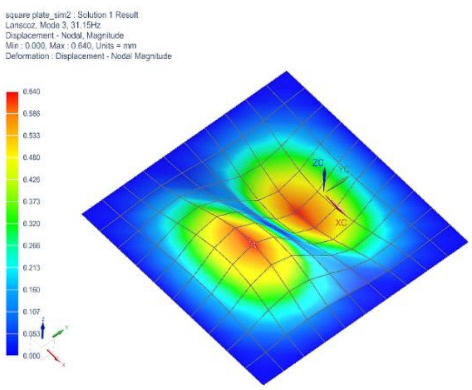	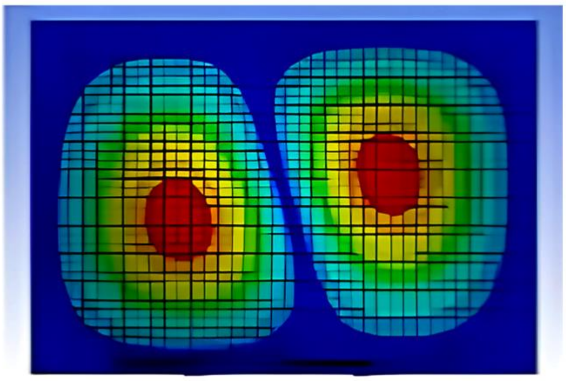

<table>
<tr><th>Mode shape of the FEA</th><th>Literature Review</th></tr>
<tr><td>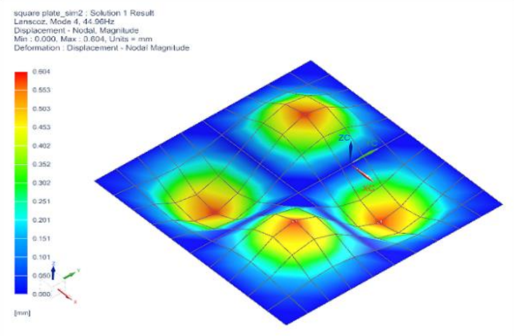
</td><td>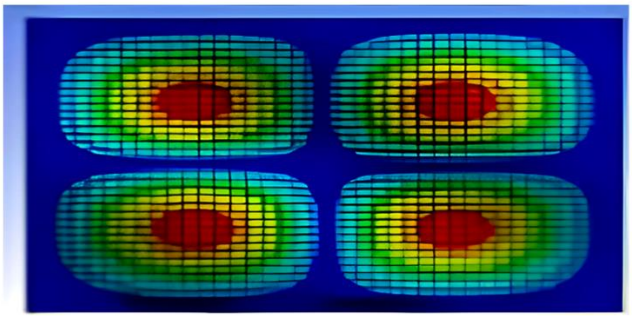</td></tr>
<tr><td>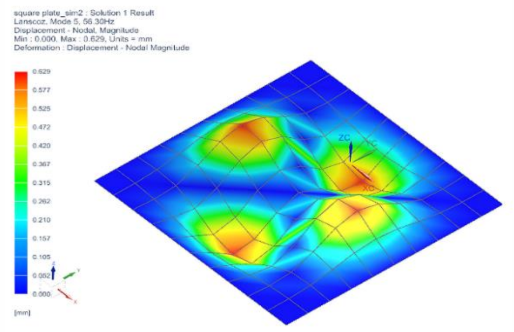
</td><td>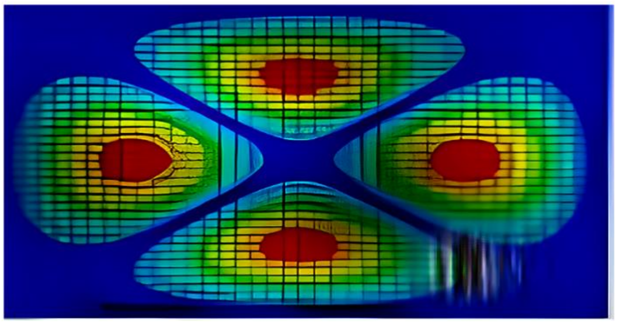</td></tr>
<tr><td>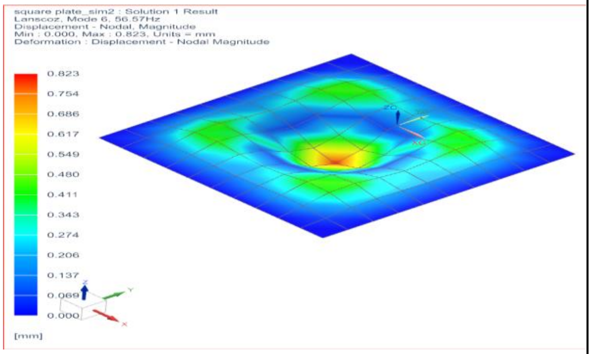
</td><td>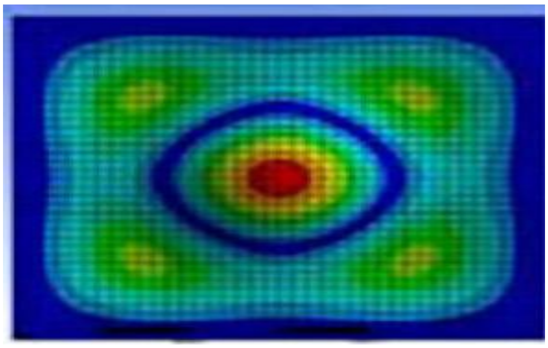</td></tr>
<tr><td>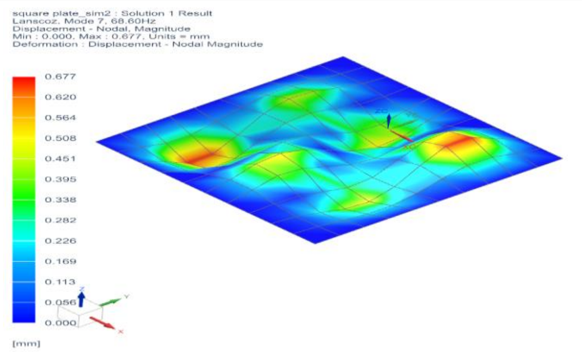
</td><td>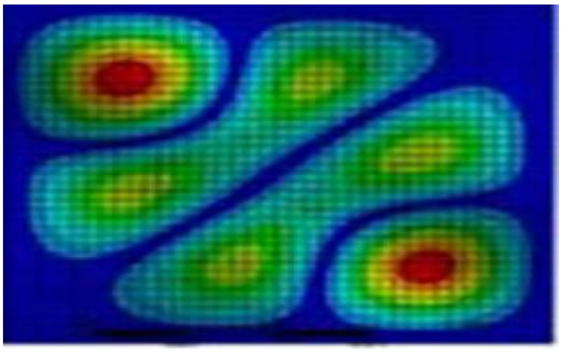</td></tr>
<tr><td>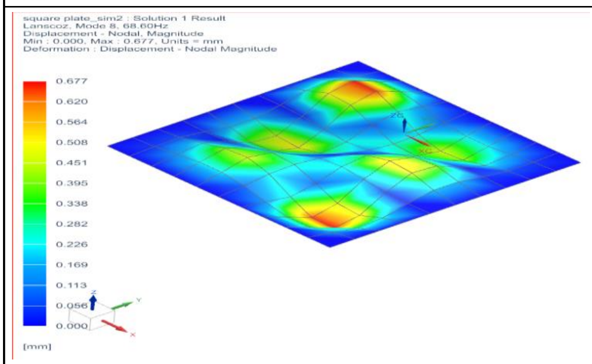
</td><td>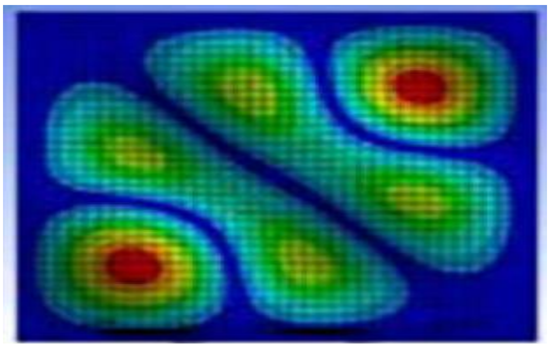</td></tr>
</table>

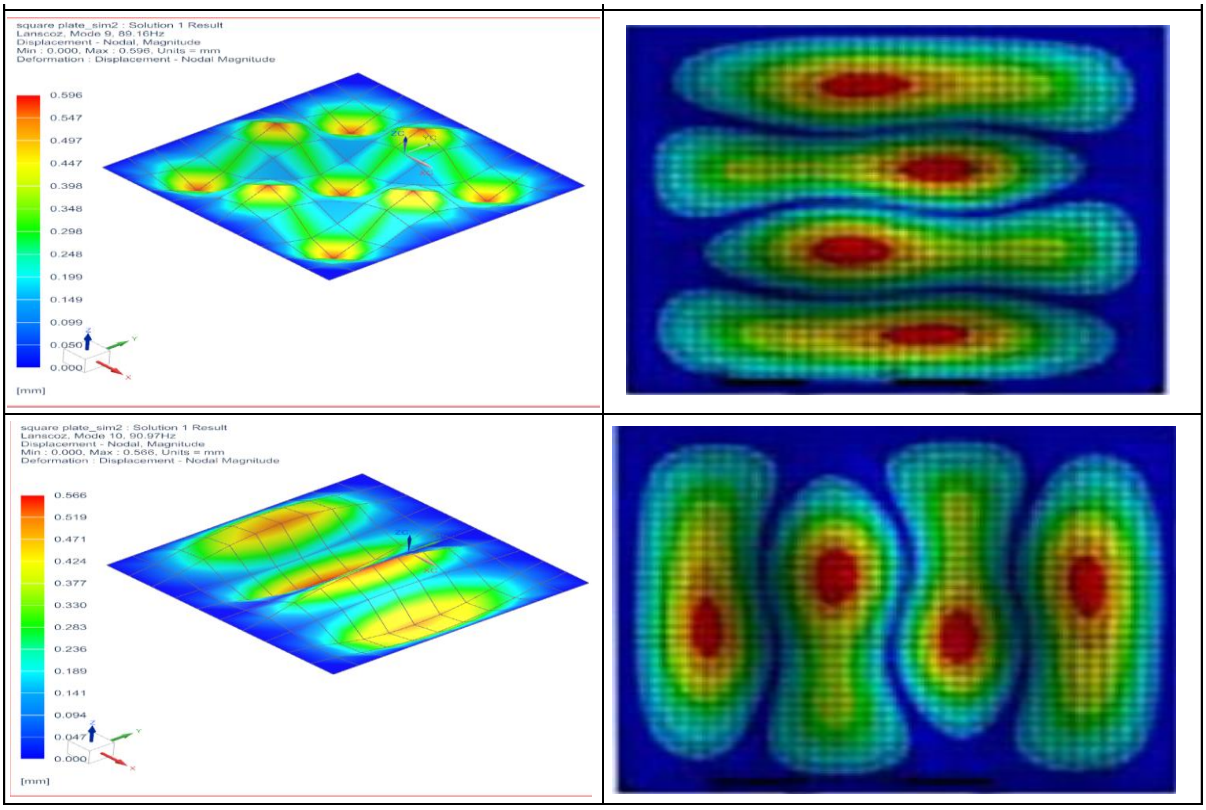

4. Conclusion

Siemens NX12's solver 103 was used to do modelling and simulation on a completely fixed plate. The findings of real Eigenvalues and analytical methods centred on Warburton's theory were paled in comparison. According to Warburton's idea, the initial frequency would generate a circular mode form on a fixed plate, which would subsequently shift as the frequency increased. Modal analysis is required in engineering since everything has a natural frequency that must be evaluated. This is because if a frequency is applied to an item that has a wavelength comparable to the frequency in the thing, both frequencies will be overlaid, leading the object to collapse, which might be harmful. Real-world examples include the Death Ray building in London and Las Vegas in 1981, the Hard rock Hotel in New Orleans, the Tacoma Narrows Bridge disaster in 1940, and a lot more. Further study may be conducted in this area to determine how natural frequencies impact a fixed plate. Earlier scholars, such as Rayleigh, whose idea was described in this study, have developed practical methods for calculating the natural frequencies inside a plate. Additional studies inside the Siemens program might be performed to examine how the findings would be influenced, such as constructing a series of meshes to determine which one delivers the most reliable data.

References

[1] Ruben Adorno, and Anthony N. Palazotto, "A Finite Element Study on the Effects of Thickness and Material Nonlinearity on the Equilibrium Path of Axially Loaded Circular Cylindrical Shells," *Engineering Structures*, vol.277, 2023. [CrossRef] [Google Scholar] [Publisher Link]

[2] Mizan Ahmed et al., "Nonlinear Analysis of Square Spiral-Confined Reinforced Concrete-Filled Steel Tubular Short Columns Incorporating Novel Confinement Model and Interaction Local Buckling," *Engineering Structures*, vol. 274, 2023. [CrossRef] [Google Scholar] [Publisher Link]

[3] Andrew Allerdt, "Many-Body Effects in Fen_4 Centre Embedded in Graphene," *Applied Sciences*, vol. 10, no. 7, pp. 1-17, 2020. [CrossRef] [Google Scholar] [Publisher Link]

[4] Klaus Jürgen Bathe, and Arthur P. Cimento, "Some Practical Procedures for the Solution of Nonlinear Finite Element Equations," *Computer Methods in Applied Mechanics and Engineering*, vol. 22, no. 1, pp. 59-85, 1980. [CrossRef] [Google Scholar] [Publisher Link]

[5] S.S. Bhavikatti, *Finite Element Analysis*, 4th ed., New Age International, 2021. [Google Scholar] [Publisher Link]

[6] Emanuele Brunesi, Roberto Nascimbene, and Gian Andrea Rassati, "Response of Partially-Restrained Bolted Beam-to-Column Connections under Cyclic Loads," *Journal of Constructional Steel Research*, vol. 97, pp. 24-38, 2014. [CrossRef] [Google Scholar] [Publisher Link]

[7] Serena Cattari et al., "Nonlinear Modeling of the Seismic Response of Masonry Structures: Critical Review and Open Issues towards Engineering Practice," *Bulletin of Earthquake Engineering*, vol. 20, no. 4, pp. 1939-1997, 2022. [CrossRef] [Google Scholar] [Publisher Link]

[8] Siu Lai Chan, "Geometric and Material Non-Linear Analysis of Beam-Columns and Frames using the Minimum Residual Displacement Method," *International Journal for Numerical Methods in Engineering*, vol. 26, no. 12, pp. 2657-2669, 1988. [CrossRef] [Google Scholar] [Publisher Link]

[9] Ashim Datta, and Vineet Rakesh, *An Introduction to Modeling of Transport Processes: Applications to Biomedical Systems*, Cambridge University Press, 2012. [Google Scholar] [Publisher Link]

[10] Ylenia Di Lallo et al., "Non-Linear Analysis of URM Structures through a Multi-Unit Discretization Approach," *Procedia Structural Integrity*, vol. 44, pp. 488-495, 2023. [CrossRef] [Google Scholar] [Publisher Link]

[11] S.M. Dickinson, and A. Di Blasio, "On the use of Orthogonal Polynomials in the Rayleigh-Ritz Method for the Study of the Flexural Vibration and Buckling of Isotropic and Orthotropic Rectangular Plates," *Journal of Sound Vibration*, vol. 108, no. 1, pp. 51-62, 1986. [CrossRef] [Google Scholar] [Publisher Link]

[12] Van Thom Do, Van Vinh Pham, and Hoang Nam Nguyen, "On the Development of Refined Plate Theory for Static Bending Behavior of Functionally Graded Plates," *Mathematical Problems in Engineering*, vol. 2020, no. 1, pp. 1-13, 2020. [CrossRef] [Google Scholar] [Publisher Link]

[13] Jian-Ping Geng, Keson B.C. Tan, and Gui-Rong Liu, "Application of finite Element Analysis in Implant Dentistry: A Review of the Literature," *The Journal of Prosthetic Dentistry*, vol. 85, no. 6, pp. 585-598, 2001. [CrossRef] [Google Scholar] [Publisher Link]

[14] Max A.N. Hendriks, and Jan G. Rots, "Sequentially Linear Versus Nonlinear Analysis of RC Structures," *Engineering Computations*, vol. 30, no. 6, pp. 792-801, 2013. [CrossRef] [Google Scholar] [Publisher Link]

[15] Sung-Min Hong, and Jae-Hyung Jang, "Numerical Simulation of Plasma Oscillation in 2-D Electron Gas using a Periodic Steady-State Solver," *IEEE Transactions on Electron Devices*, vol. 62, no. 12, pp. 4192-4198, 2015. [CrossRef] [Google Scholar] [Publisher Link]

[16] Thomas J.R. Hughes, and T.E. Tezduyar, "Finite Elements based Upon Mindlin Plate Theory with Particular Reference to the Four-Node Bilinear Isoparametric Element," *Journal of Applied Mechanics*, vol. 48, no. 3, pp. 587-596, 1981. [CrossRef] [Google Scholar] [Publisher Link]

[17] Yanchuan Hui et al., "A Geometrically Nonlinear Analysis through Hierarchical One-Dimensional Modelling of Sandwich Beam Structures," *Acta Mechanica*, vol. 234, no. 1, pp. 67-83, 2022. [CrossRef] [Google Scholar] [Publisher Link]

[18] C.C. Ike, "Ritz Variational Method for the Flexural Analysis of Rectangular Kirchhoff Plate on Winkler Foundation," 2019. [Google Scholar]

[19] Erdem Imrak, and Cuneyt Fetvaci, "The Deflection Solution of a Clamped Rectangular Thin Plate Carrying Uniformly Load," *Mechanics based Design of Structures and Machines*, vol. 37, no. 4, pp. 462-474, 2009. [CrossRef] [Google Scholar] [Publisher Link]

[20] Muhammad Imran, Rafiullah Khan, and Saeed Badshah, "Investigating the Effect of Delamination Size, Stacking Sequences and Boundary Conditions on the Vibration Properties of Carbon Fiber Reinforced Polymer Composite," *Materials Research*, vol. 22, no. 2, pp. 1-7, 2019. [CrossRef] [Google Scholar] [Publisher Link]

[21] Cornelius Lanczos, "An Iteration Method for the Solution of the Eigenvalue Problem of Linear Differential and Integral Operators," *Journal of Research of the National Bureau of Standards*, vol. 45, no. 4, pp. 255-282, 1950. [Google Scholar]

[22] Zhou Ding, "Natural Frequencies of Rectangular Plates using a Set of Static Beam Functions in Rayleigh-Rtiz Method," *Journal of Sound and Vibration*, vol. 189, no. 1, pp. 81-87, 1996. [CrossRef] [Google Scholar] [Publisher Link]

[23] Shengya Li et al., "A Highly Efficient Multi-Scale Approach of Locally Refined Nonlinear Analysis for Large Composite Structures," *Composite Structures*, vol. 306, 2023. [CrossRef] [Google Scholar] [Publisher Link]

[24] Jaroslav Mackerle, "Finite Element Linear and Nonlinear, Static and Dynamic Analysis of Structural Elements: A Bibliography (1992-1995)," *Engineering Computations*, vol. 14, no. 4, pp. 347-440, 1997. [CrossRef] [Google Scholar] [Publisher Link]

[25] Andrea Nanetti, and Davide Benvenuti, "Engineering Historical Memory and the Interactive Exploration of Archival Documents: The Online Application for Pope Gregory X's Privilege for the Monastic Community of Mount Sinai (1274) as a Prototype," *Umanistica Digitale*, vol. 10, no. 5, pp. 325-357, 2021. [Google Scholar] [Publisher Link]

[26] Witold Nowacki, *Dynamics of Elastic Systems*, Wiley, 1963. [Google Scholar]

[27] I.U. Ojalvo, and Miya Newman, "Vibration Modes of Large Structures by an Automatic Matrix-Reductionmethod," *AIAA Journal*, vol. 8, no. 7, pp. 1234-1239, 1970. [CrossRef] [Google Scholar] [Publisher Link]

[28] Chukwuemeka Joshua Okafor, "Energy Generation in Nigeria: A Literature Review," *Journal of Environmental Engineering and Energy*, vol. 1, no. 1, pp. 59-70, 2024. [CrossRef] [Publisher Link]

[29] Chukwuemeka Joshua Okafor, "Geometric Analysis of Gutter Bracket using Different NX Siemens Solver for Linear and Nonlinear Investigation," *Complexity Analysis and Applications*, vol. 2, no. 1, pp. 1-11, 2025. [CrossRef] [Publisher Link]

[30] Chukwuemeka Joshua Okafor, Adedayo Ayomide Adeniran, and Adetayo Olaniyi Adeniran, "Machine Learning and AI for Predictive Maintenance and Grid Integration of Wind Farms," *Soft Computing Fusion with Applications*, vol. 2, no. 2, pp. 62-73, 2025. [CrossRef] [Google Scholar] [Publisher Link]

[31] N.N. Osadebe, "Differential Equations for Small Deflection Analysis of Thin Elastic Plates Possessing Extensible Middle Surface," *University of Nigeria Virtual Library*, 1997. [Google Scholar]

[32] Junuthula Narasimha Reddy, "A Refined Nonlinear Theory of Plates with Transverse Shear Deformation," *International Journal of Solids and Structures*, vol. 20, no. 9-10, pp. 881-896, 1984. [CrossRef] [Google Scholar] [Publisher Link]

[33] J. Sau, and K. Heyde, “On a Comparison between Lanczos and Householder Methods,” *Journal of Physics G: Nuclear Physics*, vol. 5, no. 12, pp. 1643-1647, 1979. [CrossRef] [Google Scholar] [Publisher Link]

[34] Eftychios Sifakis, and Jernej Barbic, “FEM Simulation of 3D Deformable Solids: A Practitioner's Guide to Theory, Discretization and Model Reduction,” *ACM SIGGRAPH 2012 COURSES*, pp. 1-50, 2012. [CrossRef] [Google Scholar] [Publisher Link]

[35] Yuan Tang, and Hai Qing, “Size-Dependent Nonlinear Post-Buckling Analysis of Functionally Graded Porous Timoshenko Microbeam with Nonlocal Integral Models,” *Communications in Nonlinear Science and Numerical Simulation*, vol. 116, 2023. [CrossRef] [Google Scholar] [Publisher Link]

[36] Geoffrey B. Warburton, and S.L. Edney, “Vibrations of Rectangular Plates with Elastically Restrained Edges,” *Journal of Sound and Vibration*, vol. 95, no. 4, pp. 537-552, 1984. [CrossRef] [Google Scholar] [Publisher Link]

[37] Adanna Welch-Phillips et al., “What is Finite Element Analysis?,” *Clinical Spine Surgery*, vol. 33, no. 8, pp. 323-324, 2020. [CrossRef] [Google Scholar] [Publisher Link]

[38] Thomas H. Williamson, *Uveitis and Allied Disorders*, Vitreoretinal Surgery, Springer, pp. 505-536, 2021. [CrossRef] [Google Scholar] [Publisher Link]

[39] Yi Xue et al., “Nonlinear Mechanical Characteristics and Damage Constitutive Model of Coal under CO_2 Adsorption during Geological Sequestration,” *Fuel*, vol. 331, 2023. [CrossRef] [Google Scholar] [Publisher Link]

[40] Bing Zhao et al., “A Nonlinear Uniaxial Stress-Strain Constitutive Model for Viscoelastic Membrane Materials,” *Polymer Testing*, vol. 90, 2020. [CrossRef] [Google Scholar] [Publisher Link]

[41] Zhou Ding, “Natural Frequencies of Elastically Restrained Rectangular Plates using a Set of Static Beam Functions in the Rayleigh-Ritz Method,” *Computers & Structures*, vol. 57, no. 4, pp. 731-735, 1995. [CrossRef] [Google Scholar] [Publisher Link]